Magn Reson Med Sci 2018; 17; 318–324
doi:10.2463/mrms.mp.2017-0149
Published Online: February 13, 2018

MAJOR PAPER

# Water Diffusion in the Brain of Chronic Hypoperfusion Model Mice: A Study Considering the Effect of Blood Flow

Takuya Urushihata[1,2], Hiroyuki Takuwa[1], Chie Seki[1], Yasuhiko Tachibana[1], Manami Takahashi[1], Jeff Kershaw[1], Yuhei Takado[1], Ichio Aoki[1], Makoto Higuchi[1], Hiroshi Ito[3], and Takayuki Obata[1*]

**Purpose:** Chronic cerebral hypoperfusion model mice were created by unilateral common carotid artery occlusion (UCCAO) surgery, which does not cause cerebral infarction, but which does cause long-term reduction in cerebral blood flow (CBF) to the occluded side. Cognitive dysfunction in this mouse model has been demonstrated in behavioral experiments, but neuron density change was not found in a previous positron emission tomography (PET) study. As a next step, in this study we investigated the injury of neuronal fibers in chronic cerebral hypoperfusion model mice using diffusion tensor imaging (DTI).

**Methods:** In diffusion-weighted imaging (DWI), not only the diffusion of water but also the capillary flow in the voxel, i.e., intravoxel incoherent motion (IVIM), contributes to the signal. Thus, we used DTI to evaluate DWI signal changes in the brains of chronic hypoperfusion model mice at 4 weeks after UCCAO while monitoring the possible influence of CBF change using arterial spin-labeling (ASL) MRI.

**Results:** Simple *t*-tests indicated that there were significant differences in CBF between the control and occluded sides of the brain, but there was no significant difference for the mean diffusivity (MD) or fractional anisotropy (FA). However, as Pearson correlation analysis showed that MD was strongly correlated with CBF, analysis-of-covariance (ANCOVA) was then performed using CBF as a covariate and a significant difference in MD between the contra- and ipsilateral sides was found. Performing a similar procedure for the FA found no significant differences.

**Conclusion:** The results suggest the injury of neuronal fibers due to chronic hypoperfusion. It is also suggested that CBF-related signal changes should be considered when DWI-based information is used for pathological diagnosis.

**Keywords:** *arterial spin labeling, chronic cerebral hypoperfusion, diffusion tensor imaging, intravoxel incoherent motion, mean diffusivity*

## Introduction

Vascular dementia (VaD) is the second most common type of dementia after Alzheimer's disease. Although it is known that VaD is usually caused by both wide-range and local cerebral infarction, it can also be induced by hypoperfusion. However, the mechanism behind cognitive dysfunction due to hypoperfusion is not well understood. Model animals are often used to study VaD resulting from hypoperfusion. A rat model of bilateral occlusion of the common carotid arteries (BCCAO) showed white matter lesions, such as demyelination and increased astroglia, and declined working memory performance when negotiating a water maze.[1–6] Even in a mouse model of right unilateral common carotid artery occlusion (UCCAO), white matter lesions and deficits of memory ability in object-recognition have been reported.[7] We previously demonstrated a mouse model of misery perfusion due to permanent UCCAO,[8] and subsequent studies using positron emission tomography (PET) and immunostaining showed that neuron density did not significantly change at 28 days after surgery.[9] These results suggest that injury of neuronal fibers, rather than cell death, may be the cause of cognitive dysfunction in this mouse model.

[1]National Institute of Radiological Sciences, National Institutes for Quantum and Radiological Science and Technology, 4-9-1 Anagawa, Chiba, Chiba 263-8555, Japan
[2]United Graduate School of Agricultural Science, Iwate University, Iwate, Japan
[3]Department of Radiology and Nuclear Medicine, Fukushima Medical University, Fukushima, Japan

*Corresponding author, Phone: +81-43-206-3203,
E-mail: obata.takayuki@qst.go.jp



Received: October 17, 2017 | Accepted: December 20, 2017

Diffusion tensor imaging (DTI) has been used as an important tool for evaluating injury of neuronal fibers.[10,11] So far, research on chronic hypoperfusion with DTI has been conducted in rat models of BCCAO.[12,13] Although the results for the optic nerve and optic tract were similar for those two studies, the DTI measurements in the cortex, hippocampus, and white matter relative to cognitive function were not consistent. One of the studies found no change to the mean diffusivity (MD) in the cortex,[13] while the other showed an increase in MD.[12] This difference may be caused by changes to cerebral blood flow (CBF) during DTI measurements. In diffusion-weighted imaging (DWI), not only the diffusion of water but also the capillary flow in the voxel, i.e. intravoxel incoherent motion (IVIM), contributes to the signal attenuation.[14–17] It has been shown that IVIM parameter estimates and arterial spin-labeling (ASL)-based estimates of blood flow behave in a similar way.[18–22] It has been reported that the IVIM pseudo diffusion coefficient (D*) and CBF measured with ASL show a positive correlation,[18,19] and that a decrease in blood flow due to cirrhosis causes a decrease in D*.[22] Therefore, in animal models of conditions where changes in blood flow can occur, such as chronic hypoperfusion, it is possible that both neuronal injury and blood flow changes may affect the results of DTI.

In this study, we used DTI to evaluate water diffusion changes in the brains of chronic hypoperfusion model mice while monitoring the possible influence of CBF change using ASL MRI. In addition, immunostaining of *ex vivo* brain sections was conducted to validate the results of DTI.

## Materials and Methods

### *Animal preparation*

A total of 10 male C57BL/6J mice (20–30 g, 8–10 weeks; Japan SLC Inc., Hamamatsu, Japan) were used in the diffusion MRI experiments. All mice were housed individually in separate cages with water and food *ad libitum*. Mouse cages were kept at a temperature of 25°C in a 12-h light/dark cycle.

For the UCCAO surgical procedure, a mixture of air, oxygen, and isoflurane (3–5% for induction and 1.5–2% for surgery) anesthesia was given by face mask. A midline cervical incision was made and the right common carotid artery was isolated from the adjacent vagus nerve and double-ligated using 6–0 silk sutures.

All animal experiments were approved by the Institutional Animal Care and Use Committee of the National Institute of Radiological Sciences (Chiba, Japan) and were performed in accordance with the institutional guidelines on human care and use of laboratory animals approved by the Institutional Committee for Animal Experimentation.

### *Magnetic resonance imaging measurements*

The MRI measurements were performed at 4 weeks after UCCAO on a 7T animal MRI system (Kobelco and Bruker, Tokyo, Japan). The mice were initially anesthetized with 3.0% isoflurane (Escain; Mylan Japan, Tokyo, Japan) and then with 1.5–2.0% isoflurane and a 1:5 oxygen/room-air mixture during the MRI experiments. Rectal temperature was continuously monitored by optical fiber thermometer (FOP-M; FISO, Quebec, QC, Canada) and maintained at 37.0 ± 0.5°C using a heating pad (Temperature control unit; RAPID Biomedical GmbH, Rimpar, Germany). Warm air was provided with a homemade automatic heating system regulated by an electric temperature controller (E5CN; OMRON Corporation, Kyoto, Japan) throughout all experiments. During MRI scanning, the mice lay in a prone position on an MRI-compatible cradle and were held in place with handmade ear bars.

The DTI was performed with a 4-shot spin-echo echo-planar imaging (EPI) sequence (TR = 3.5 s, TE = 23 ms, FOV = 2.56 cm × 2.56 cm, matrix size = 128 × 128, slice thickness = 1 mm, gradient directions = 30, $\Delta$ = 10 ms, $\delta$ = 5 ms). Imaging was performed at b value = 0 and 670 s/mm$^2$, where the lager value is the default of the used MR system.

The CBF measurements were carried out using the flow-sensitive alternating inversion recovery (FAIR) ASL technique with rapid acquisition with relaxation enhancement (RARE) image acquisition (TR = 12 s, TR = 46.8 ms, FOV = 2.56 cm × 2.56 cm, matrix size = 128 × 128, slice thickness = 1 mm, and RARE factor = 72). For both non-selective and slice-selective acquisitions, images at 22 different inversion times (TIs) were acquired: 30, 100, 200, 300, 400, 500, 600, 700, 800, 900, 1000, 1100, 1200, 1300, 1400, 1500, 1600, 1700, 1800, 1950, 2100, and 2300 ms. Quantitative traveling-time-independent CBF values were calculated from the signal differences between the non-selective and slice-selective images at all TIs.[23]

### *DTI and CBF data processing*

An ordinary least-squares method was used to estimate the diffusion tensor on a voxel-by-voxel basis with software written in MatLab (The MathWorks, Inc., Natick, MA, USA). The eigenvalues ($\lambda 1$, $\lambda 2$, and $\lambda 3$) of the diffusion tensor were used to calculate the MD and fractional anisotropy (FA) as defined by the following equations:

$$\mathrm{MD} = (\lambda 1 + \lambda 2 + \lambda 3)/3 \quad (1)$$

$$\mathrm{FA} = \sqrt{\frac{3}{2}}\sqrt{\frac{(\lambda 1 - \mathrm{MD})^2 + (\lambda 2 - \mathrm{MD})^2 + (\lambda 3 - \mathrm{MD})^2}{\lambda 1^2 + \lambda 2^2 + \lambda 3^2}} \quad (2)$$

Regions-of-interest in the dorsal cortex, corpus callosum with external capsule (CC + EC), and hippocampus were manually drawn on the FA maps from each animal (Fig. 1B), and the average values of the CBF, MD, and FA were calculated for each ROI.

### *Statistical analysis*

Statistical analyses were performed with the Statistics and Machine Learning Toolbox of MatLab. All values are presented as mean ± standard deviation in the "Results" section. At first, the difference in MD and FA between the contralateral

and ipsilateral sides was tested with a paired *t*-test. Since a positive correlation between CBF and D* has been reported,[18,22] Pearson correlation analysis was performed between CBF and DTI estimates. Differences in MD and FA between the ipsilateral (common-carotid-artery occluded [CCAO]) and contralateral sides were then analyzed with analysis of covariance (ANCOVA) using the CBF as a covariate. A $P$-value < 0.05 was interpreted as being statistically significant.

### *Corrected MD or FA map*

Corrected MD and FA maps were created when ANCOVA was found to have a significant effect. The correction method is explained here for the MD map (it can also apply to FA). First, the MD map from one animal was selected as a template, and the maps from the remaining animals were registered to it using the Image Processing Toolbox of MatLab. Second, using the data from all animals, for each pixel the slope (Slope ($Xi$, $Yj$)) of the regression line of MD to CBF was estimated by ordinary least-squares. The mean MD ($MD_{ave}(Xi, Yj)$) and corrected MD ($MD_{corr}(Xi, Yj)$) for each pixel were then obtained using the following equations:

$$MD_{ave}(Xi, Yj) = \frac{1}{n}\sum_{k=1}^{n} MD_k(Xi, Yj) \quad (3a)$$

$$MD_{corr}(Xi, Yj) = \frac{1}{n}\sum_{k=1}^{n}(MD_k(Xi, Yj) + CBF_{ave} - CBF_k(Xi, Yj)) \times Slope(Xi, Yj)) \quad (3b)$$

where $CBF_{ave}$ is the approximate average value of CBF in the dorsal cortex and CC + EC.

### *Histology and immunohistochemistry examinations*

The mice were deeply anesthetized with an intraperitoneal injection of pentobarbital (10 mg/kg) and perfused transcardially with saline. The brains were then sampled and immersed in 4% paraformaldehyde mixed with phosphate buffer saline (PBS) and kept at 4°C overnight. Thereafter, brains were immersed in a mixture of 30% sucrose and 70% PBS and kept at 4°C for 3 days. The brains were frozen and sliced into 20-μm thick coronal sections and mounted on glass slides (Matsunami Glass Ind., Ltd., Osaka, Japan). The sections were then immunolabeled against MAP2 (rabbit polyclonal, 1:1,000; Cell Signaling Technology Japan, K.K., Tokyo, Japan) and kept at 4°C overnight. The sections were washed three times in PBS for 5 min and then incubated with anti-rabbit IgG biotin (1:1,000) for 1 h at room temperature. Finally, immunoreactivity was visualized using fluorescein-labeled tyramide signal amplification (PerkinElmer Japan Co., Ltd, Kanagawa, Japan).

## Results

### *Comparison of ipsilateral and contralateral measurements with a paired t-test*

Brain injury after UCCAO was not observed on the $T_2$-weighted images (Fig. 1A). Clear CBF, MD, and FA

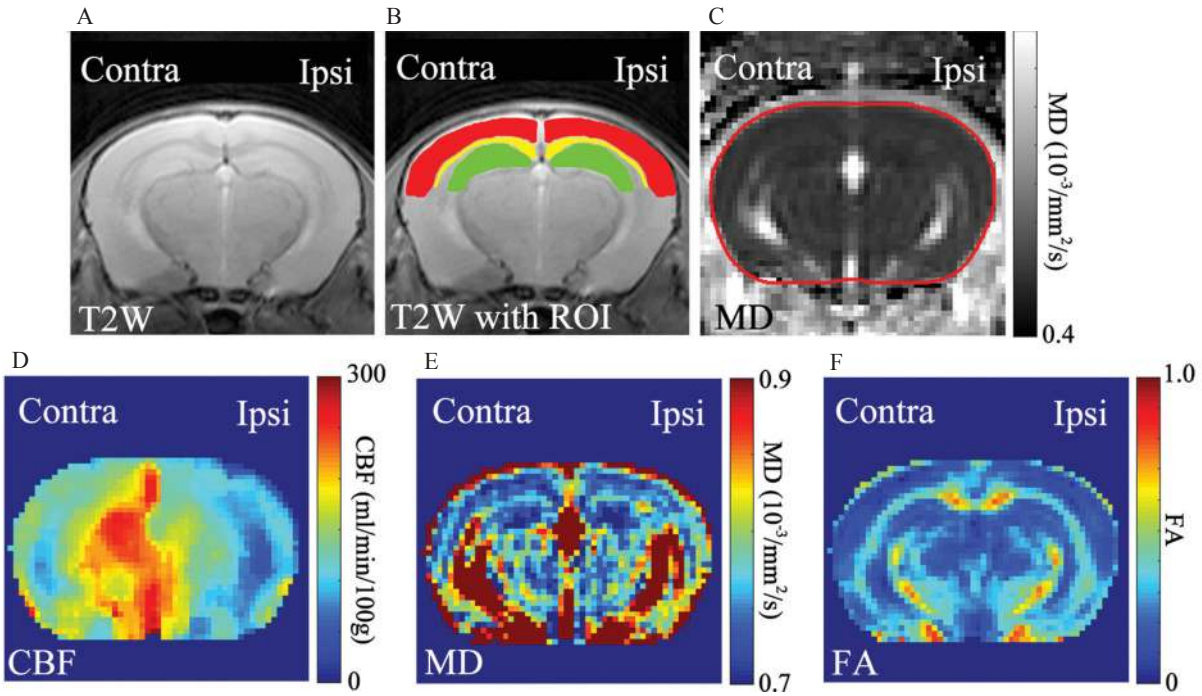


**Fig. 1** (**A**) $T_2$-weighted image of a chronic hypoperfusion model mouse (UCCAO). (**B**) $T_2$-weighted image with dorsal cortex (red), corpus callosum with external capsule (CC + EC, yellow) and hippocampus (green) ROIs drawn on both the ipsilateral side (right) and contralateral side (left) of the brain. (**C**) Mean diffusivity (MD) map showing the selected brain region outlined in red. (**D**–**F**) Typical cerebral blood flow (CBF) (**D**), MD (**E**), and fractional anisotropy (FA) (**F**) maps from a chronic hypoperfusion model mouse (UCCAO).The CBF map has left-right asymmetry, but the MD and FA maps look more symmetric.

maps of all mouse brains at 4 weeks after UCCAO were obtained (Fig. 1C-1F). Significant changes between the ipsilateral and contralateral regions were analyzed with a paired *t*-test. For CBF (Fig. 2A), the ipsilateral side showed a significant reduction compared to the contralateral side in the dorsal cortex, CC + EC and hippocampus ROIs (paired *t*-test: $P < 0.001$). On the other hand, neither MD (Fig. 2B) nor FA (Fig. 2C) showed a significant difference for any of the ROIs.

### *Pearson correlation analysis between the CBF and DTI estimates*

Pearson correlation analysis showed that CBF and MD in the dorsal cortex were positively correlated on both the ipsilateral ($r = 0.866$, $P < 0.001$) and contralateral ($r = 0.644$, $P < 0.001$) sides of the brain (Fig. 3A). Positive correlations were also confirmed for both sides in the CC + EC (Fig. 3B, $r = 0.812$ and 0.667, $P < 0.001$) and hippocampus (Fig. 3C, $r = 0.455$ and 0.714, $P < 0.01$). Similar analysis showed no correlation between CBF and FA in the dorsal cortex for either the ipsilateral ($r = 0.0115$) or the contralateral sides ($r = -0.104$). Similarly, there was no correlation on either side for CC + EC ($r = 0.0954$ and 0.301) and hippocampus ($r = 0.239$ and 0.194).

### *Comparison of ipsilateral and contralateral measurements using ANCOVA*

Prompted by these results, MD and FA were then analyzed with ANCOVA using the CBF as a covariate. Analysis-of-covariance revealed significant differences in MD between the ipsilateral and contralateral sides of both the dorsal cortex (interaction CBF × CCAO, $P = 0.408$; CBF effect, $F = 22.5$, $P = 0.0002$; CCAO effect, $F = 9.45$, $P = 0.0073$), and CC + EC ROIs (interaction CBF × CCAO, $P = 0.728$; CBF effect, $F = 20.9$, $P = 0.0003$; CCAO effect, $F = 16.9$, $P = 0.0008$). In the hippocampus, even though MD and CBF were positively correlated for both sides (Fig. 3C), ANCOVA found no significant CCAO effect (interaction CBF × CCAO, $P = 0.728$; CBF effect, $F = 10.3$, $P = 0.0056$; CCAO effect, $F = 1.23$, $P = 0.284$). ANCOVA found neither a significant CBF nor CCAO effect in FA for all regions (dorsal cortex: interaction CBF × CCAO, $P = 0.969$;

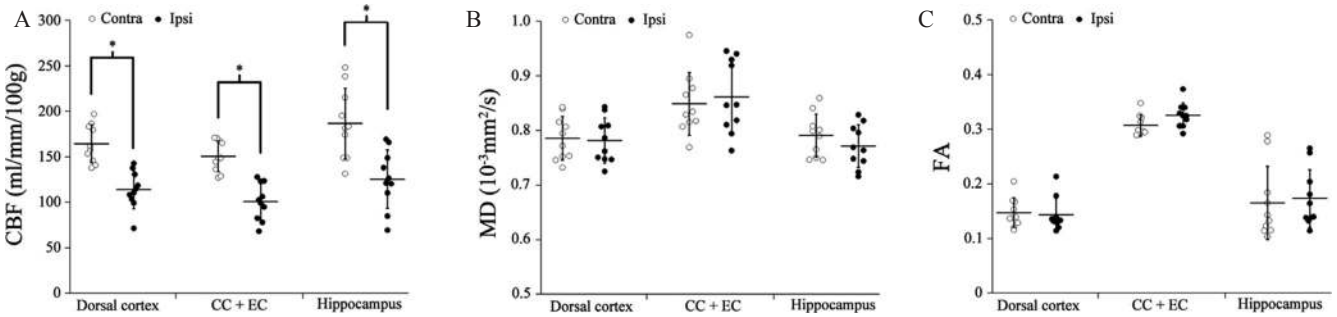


**Fig. 2** Average values with standard deviations of cerebral blood flow (CBF) (**A**), mean diffusivity (MD) (**B**), and fractional anisotropy (FA) (**C**) in the dorsal cortex, corpus callosum with external capsule (CC + EC) and hippocampus ROIs. The open and closed circles indicate the average values on the occluded and contralateral sides, respectively, of each mouse. Significant reduction of CBF on the occluded side was found for all three ROIs ($P < 0.001$), while neither MD nor FA showed a significant difference for any of the ROIs. *$P < 0.05$.

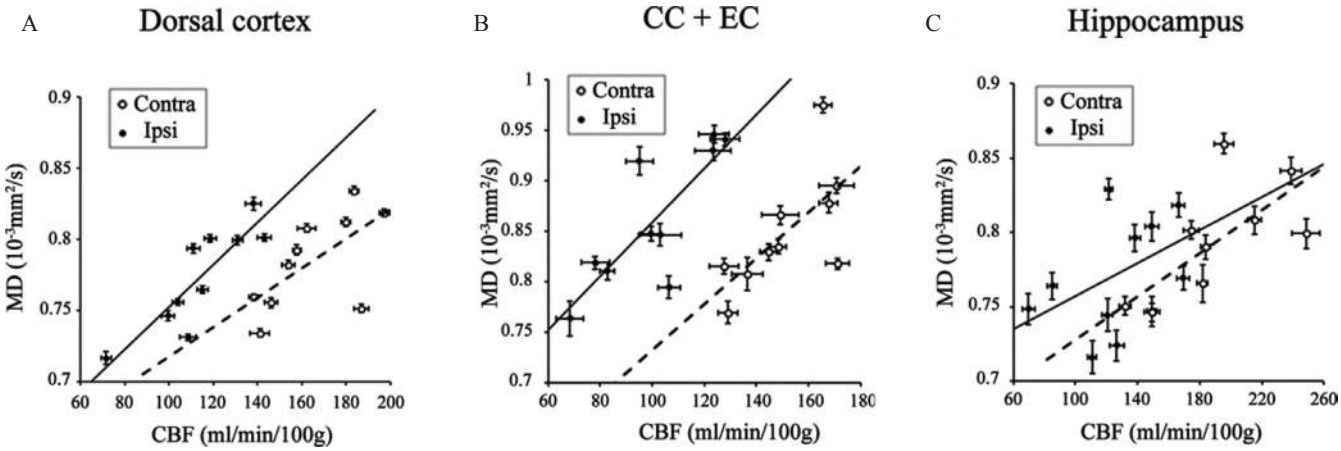


**Fig. 3** Mean diffusivity (MD) plotted against cerebral blood flow (CBF) for dorsal cortex (**A**), corpus callosum with external capsule (CC + EC) (**B**) and hippocampus (**C**) ROIs. The straight lines are fits to MD with respect to CBF for the ipsilateral side (closed circles with standard error [SE] bars). The broken lines are similar fits for the contralateral side (open circles with SE bars). CBF and MD showed a positive correlation for all ROIs.

CBF effect, $F = 0.0898$, $P = 0.768$; CCAO effect, $F = 5.89e\text{-}5$, $P = 0.994$; CC + EC: interaction CBF × CCAO, $P = 0.0853$; CBF effect, $F = 0.116$, $P = 0.116$; CCAO effect, $F = 0.291$, $P = 0.597$; hippocampus: interaction CBF × CCAO, $P = 0.0837$; CBF effect, $F = 0.990$, $P = 0.335$; CCAO effect, $F = 0.804$, $P = 0.383$). The ANCOVA results are summarized in Table 1.

## Corrected MD Map

Based on the results of ANCOVA, we created an MD map that was corrected in consideration of the influence of blood flow (Fig. 4). In this study, the approximate value of $CBF_{ave}$ was 130 (ml/min/100 g). The corrected map, $MD_{corr}$, appeared to have a higher MD on the ipsilateral side (Fig. 4B; arrowhead). Also, in the hippocampus, the $MD_{corr}$ map appeared higher on the ipsilateral side than on the contralateral side (Fig. 4B; arrows), although ANCOVA did not show a significant difference.

### *MAP2 immunohistochemical staining*

Staining of brain sections with MAP2, which binds to the cell body and dendrites, showed a decrease in luminance on the ipsilateral side of the brain (Fig. 5). This can be best seen on the profile drawn through the brain (Fig. 5A, white dotted line) and displayed in Fig. 5B. It is clear that there is an intensity decrease on the ipsilateral side, especially in the dorsal cortex (Fig. 5B).

## Discussion

### *Effect of blood flow on DTI in mouse brain*

In this study, neuronal fiber injury in chronic hypoperfusion model mice was evaluated with DTI, and the possible influence of CBF change on DTI was investigated using ASL. Although Hu et al. have reported that a correlation between DTI and ASL was observed in the human brain of acute ischemic stroke (AIS) patients,[18] this combination of imaging techniques is rarely used for disease studies with animal models. As changes in CBF and changes in water diffusion due to neuronal injury may affect DTI parameter estimates, it is necessary to separate these two effects to accurately evaluate DTI results in a disease model.

In this study, CBF and MD showed a positive correlation in every ROI (Fig. 3), which suggests that MD was influenced by changes in CBF. Since there was significant correlation between CBF and MD, we performed a statistical analysis with ANCOVA using the CBF as a covariate (Table 1). As ANCOVA is an analytical method that can reduce the influence of selected effects by using them as covariates on the values to be compared, it is very useful for the analysis of pure MD change without a CBF effect. MD showed no change with a *t*-test, but ANCOVA found a significant increase in MD for the dorsal cortex and CC + EC of UCCAO mice. Similar analysis was performed for FA, but no significant change could be demonstrated (graph not shown).

**Table 1.** Analysis-of-covariance (ANCOVA) results (*F*-values and *P*-values) for MD and FA

| | MD | | | FA | | |
|---|---|---|---|---|---|---|
| | Dorsal cortex | CC + EC | Hippocampus | Dorsal cortex | CC + EC | Hippocampus |
| CBF x CCAO | 0.720 (0.408) | 0.130 (0.728) | 0.130 (0.728) | 0.00150 (0.969) | 0.0354 (0.853) | 0.0437 (0.837) |
| CBF effect | 22.5 (0.0002)* | 20.9 (0.0003)* | 10.3 (0.0056)* | 0.0898 (0.768) | 0.116 (0.738) | 0.990 (0.335) |
| CCAO effect | 9.45 (0.0073)* | 16.9 (0.0008)* | 1.23 (0.284) | 5.89e-5 (0.994) | 0.291 (0.597) | 0.804 (0.383) |

The numbers within parenthesis are *P*-values, and those less than 0.05 were interpreted as being statistically significant (*). CBF, cerebral blood flow; CCAO, common carotid artery occluded; CC + EC, corpus callosum and external capsule; FA, fractional anisotropy; MD, mean diffusivity.

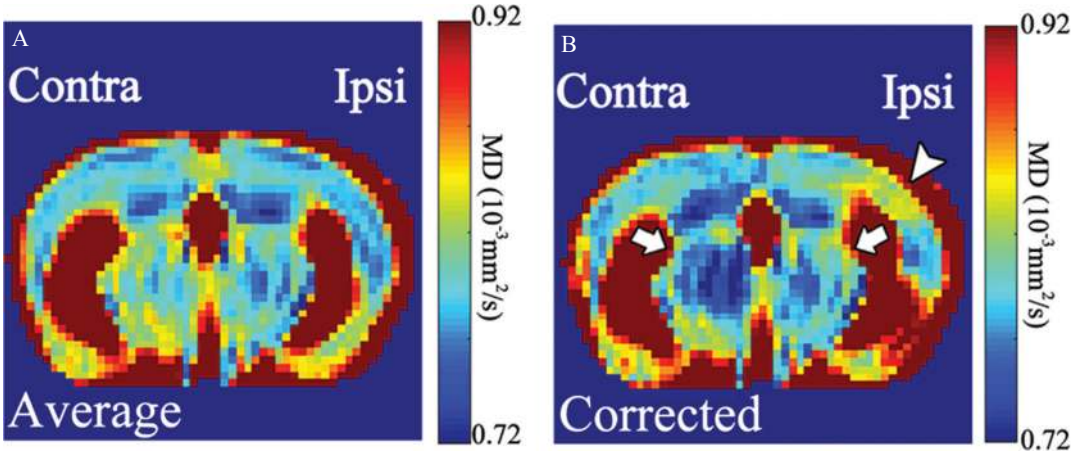


**Fig. 4** Maps of the average mean diffusivity (MD) before (**A**) and after (**B**) correction for the influence of blood flow. Mean diffusivity on the ipsilateral side appears higher than the contralateral side in dorsal cortex and corpus callosum with external capsule (CC + EC) (**B**: arrowhead). It may also be higher in the hippocampus (**B**: arrows).

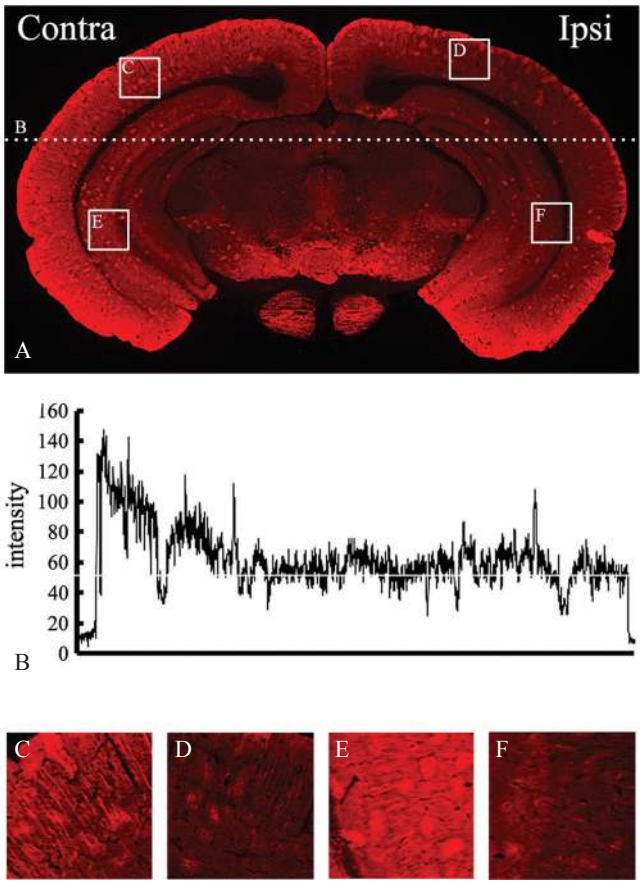


**Fig. 5** MAP2 immunohistochemical staining of a brain section. (**A**) The whole brain slice. (**B**) Image intensity along the white dotted line shown on (**A**). (**C**–**F**) Enlarged view of selected regions in the dorsal cortex (**C** and **D**) and the hippocampus (**E** and **F**). Staining of brain sections with MAP2 showed a decrease in luminance on the occlusion side.

Micro-perfusion, which produces the IVIM effect, does not have a specific flow direction (the so-called "incoherence"). On the other hand, FA is a quantity indicating the degree of diffusion anisotropy. With respect to Eq. (2) in the "Materials and Methods" section, if a change in CBF produces an increase in all three $\lambda s$ by about the same factor, it is not expected that FA will be significantly altered. In such a case, it would be reasonable that the CBF-related FA changes were only small compared to those for MD.

### *Nerve fiber degeneration due to chronic hypoperfusion*

Our DTI study found an increase in MD after UCCAO in dorsal cortex and CC + EC, and no change in hippocampus. This result is consistent with past pathology studies.[3] In a previous study with $^{11}$C-flumazenil ($^{11}$C-FMZ) PET and immunostaining with Klüver–Barrera and anti-NeuN, no neuronal death was observed after UCCAO.[9] Therefore, it is suggested that one of the causes of cognitive dysfunction in the chronic hypoperfusion model reported by behavioral experiments may be neuronal fiber injury. MAP2 immunostaining dyes cell bodies and dendrites. Since there is no change in cell body density after UCCAO,[9] the changes obtained in the present study are thought to be due to injury of dendrites (Fig. 5). The results of MAP2 immunostaining together with the other evidence presented here suggest that the increase in MD is caused by neuronal fiber injury.

In previous DTI studies of chronic hypoperfusion model rats, MD decreased[12] or did not change in white matter and cortex.[13] As the b-values they used (Soria et al.[12]: b = 1,000 and Wang et al.[13]: b = 800) are larger than that used in this study (b = 670), the effect of CBF on MD for their data may be smaller than that seen here. However, considering the fact that the CBF effect cannot be neglected at such b-values,[19] our results indicate a possibility that the reduction of MD due to CBF change masks the increase of MD caused by neuronal fiber injury. A possible means to reduce the effect of CBF on DTI parameter estimates may be to image at b = nonzero (e.g., 200 s/mm$^2$) and 1,000 s/mm$^2$, or to perform multi-b-value DWI measurements.

If the cause of MD elevation is neuronal injury, a decrease in FA might also be expected. However, FA reduction due to chronic hypoperfusion was not observed in our study. A possible reason for this can be raised. Neuronal injury due to chronic hypoperfusion is thought to accompany axonal disorders such as demyelination.[5] Also, astrogliosis and microgliosis have been reported in a chronic hypoperfusion model.[12] Such a condition may induce the formation of glial scarring after axonal damage, which has been reported to increase the FA value.[24] Therefore, reduction of FA caused by neuronal injury or demyelination may mask the FA increase caused by glial scar formation. Further studies are needed to explore the details of why FA did not show any change in this study.

### *Effect of ASL slice orientation on quantitative CBF values*

It is possible that the choice of ASL slice orientation may change the signal intensity because of differences in selected tagging arteries and in-place feeding arteries. However, the inhomogeneity of traveling time of the labeled blood in the mouse brain is smaller than that for humans, and the multi-TI ASL sequence used can reduce the dependence on travel-time.[23] Therefore, the ASL slice orientation may have little effect on the quantitative CBF value.

## Conclusion

The increase in MD after UCCAO found by ANCOVA may be due to neuronal fiber injury. This view is supported by the immunohistochemical staining results. The result that no significant difference between ipsilateral and contralateral MD was obtained with a paired *t*-test suggests that the increase in MD is masked by CBF-related signal changes. This indicates that CBF-related signal changes should be considered when using DTI for pathological diagnosis.

## Acknowledgments

The authors thank Ms. Sayaka Shibata and Mr. Nobuhiro Nitta for help with the MRI measurements. This work was supported by a Grant-in-Aid for Scientific Research (KAKENHI, #15H04910 [TO], #17J06361 [TU] and #23591809 [CS]) from the Japan Society for the Promotion of Science (JSPS), and by a grant from the Ministry of Education, Culture, Sports, Science and Technology (MEXT), Japanese Government.

## Conflicts of Interest

The authors declared no potential conflicts of interest with respect to the research, authorship and publication of this article.

## References

1. Cechetti F, Worm PV, Pereira LO, Siqueira IR, Netto AC. The modified 2VO ischemia protocol causes cognitive impairment similar to that induced by the standard method, but with a better survival rate. Braz J Med Biol Res 2010; 43:1178–1183.
2. Shibata M, Ohtani R, Ihara M, Tomimoto H. White matter lesions and glial activation in a novel mouse model of chronic cerebral hypoperfusion. Stroke 2004; 35:2598–2603.
3. Shibata M, Yamasaki N, Miyakawa T, et al. Selective impairment of working memory in a mouse model of chronic cerebral hypoperfusion. Stroke 2007; 38:2826–2832.
4. Wakita H, Tomimoto H, Akiguchi I, et al. Glial activation and white matter changes in the rat brain induced by chronic cerebral hypoperfusion: an immunohistochemical study. Acta Neuropathol 1994; 87:484–492.
5. Wakita H, Tomimoto H, Akiguchi I, et al. Axonal damage and demyelination in the white matter after chronic cerebral hypoperfusion in the rat. Brain Res 2002; 924:63–70.
6. Kurumatani T, Kudo T, Ikura Y, Takeda M. White matter changes in the gerbil brain under chronic cerebral hypoperfusion. Stroke 1998; 29:1058–1062.
7. Yoshizaki K, Adachi K, Kataoka S, et al. Chronic cerebral hypoperfusion induced by right unilateral common carotid artery occlusion causes delayed white matter lesions and cognitive impairment in adult mice. Exp Neurol 2008; 210:585–591.
8. Tajima Y, Takuwa H, Kokuryo D, et al. Changes in cortical microvasculature during misery perfusion measured by two-photon laser scanning microscopy. J Cereb Blood Flow Metab 2014; 34:1363–1372.
9. Nishino A, Tajima Y, Takuwa H, et al. Long-term effects of cerebral hypoperfusion on neural density and function using misery perfusion animal model. Sci Rep 2016; 6:25072.
10. Abe O, Aoki S, Hayashi N, et al. Normal aging in the central nervous system: quantitative MR diffusion-tensor analysis. Neurobiol Aging 2002; 23:433–441.
11. Taoka T, Fujioka M, Kashiwagi Y, et al. Time course of diffusion kurtosis in cerebral infarctions of transient middle cerebral artery occlusion rat model. J Stroke Cerebrovasc Dis 2016; 25:610–617.
12. Soria G, Tudela R, Márquez-Martín A, et al. The ins and outs of the BCCAo model for chronic hypoperfusion: a multimodal and longitudinal MRI approach. PLoS ONE 2013; 8:e74631.
13. Wang X, Lin F, Gao Y, Lei H. Bilateral common carotid artery occlusion induced brain lesions in rats: A longitudinal diffusion tensor imaging study. Magn Reson Imaging 2015; 33:551–558.
14. Le Bihan D, Breton E, Lallemand D, Grenier P, Cabanis E, Laval-Jeantet M. MR imaging of intravoxel incoherent motions: application to diffusion and perfusion in neurologic disorders. Radiology 1986; 161:401–407.
15. Le Bihan D, Breton E, Lallemand D, Aubin ML, Vignaud J, Laval-Jeantet M. Separation of diffusion and perfusion in intravoxel incoherent motion MR imaging. Radiology 1988; 168:497–505.
16. Iima M, Yano K, Kataoka M, et al. Quantitative non-Gaussian diffusion and intravoxel incoherent motion magnetic resonance imaging: differentiation of malignant and benign breast lesions. Invest Radiol 2015; 50:205–211.
17. Ichikawa S, Motosugi U, Hernando D, et al. Histological grading of hepatocellular carcinomas with intravoxel incoherent motion diffusion-weighted imaging: inconsistent results depending on the fitting method. Magn Reson Med Sci 2017 August 16. 2017. doi.org/10.2463/mrms.mp.2017-0047. [Epub ahead of print]
18. Hu LB, Hong N, Zhu WZ. Quantitative measurement of cerebral perfusion with intravoxel incoherent motion in acute ischemia stroke: initial clinical experience. Chin Med J 2015; 128:2565–2569.
19. Shen N, Zhao L, Jiang J, et al. Intravoxel incoherent motion diffusion-weighted imaging analysis of diffusion and microperfusion in grading gliomas and comparison with arterial spin labeling for evaluation of tumor perfusion. J Magn Reson Imaging 2016; 44:620–632.
20. Lin Y, Li J, Zhang Z, et al. Comparison of intravoxel incoherent motion diffusion-weighted MR imaging and arterial spin labeling MR imaging in gliomas. Biomed Res Int 2015; 2015:234245.
21. Zhang X, Ingo C, Teeuwisse WM, Chen Z, van Osch MJP. Comparison of perfusion signal acquired by arterial spin labeling-prepared intravoxel incoherent motion (IVIM) MRI and conventional IVIM MRI to unravel the origin of the IVIM signal. Magn Reson Med 2017; 79:723–729.
22. Patel J, Sigmund EE, Rusinek H, Oei M, Babb JS, Taouli B. Diagnosis of cirrhosis with intravoxel incoherent motion diffusion MRI and dynamic contrast-enhanced MRI alone and in combination: preliminary experience. J Magn Reson Imaging 2010; 31:589–600.
23. Kim SG. Quantification of relative cerebral blood flow change by flow-sensitive alternating inversion recovery (FAIR) technique: application to functional mapping. Magn Reson Med 1995; 34:293–301.
24. Kennedy PG. Postmortem survival characteristics of rat glial cells in culture. J Neurol Neurosurg Psychiatry 1987; 50:798–800.